Proc. Natl. Acad. Sci. USA
Vol. 93, pp. 7512–7517, July 1996
Biochemistry

Intermolecular disulfide bonds stabilize VirB7 homodimers and VirB7/VirB9 heterodimers during biogenesis of the *Agrobacterium tumefaciens* T-complex transport apparatus

(conjugation/lipoprotein/covalent cross-linking/macromolecular assembly)

GIULIETTA M. SPUDICH, DAVID FERNANDEZ, XUE-RONG ZHOU, AND PETER J. CHRISTIE*

Department of Microbiology and Molecular Genetics, The University of Texas Health Science Center, Houston, TX 77030

Communicated by Eugene W. Nester, University of Washington School of Medicine, Seattle, WA, April 25, 1996 (received for review February 26, 1996)

ABSTRACT **The *Agrobacterium tumefaciens* VirB7 lipoprotein contributes to the stabilization of VirB proteins during biogenesis of the putative T-complex transport apparatus. Here, we report that stabilization of VirB7 itself is correlated with its ability to form disulfide cross-linked homodimers via a reactive Cys-24 residue. Three types of β-mercaptoethanol-dissociable complexes were visualized with VirB7 and/or a VirB7::PhoA41 fusion protein: (*i*) a 9-kDa complex corresponding in size to a VirB7 homodimer, (*ii*) a 54-kDa complex corresponding in size to a VirB7/VirB7::PhoA41 mixed dimer, and (*iii*) a 102-kDa complex corresponding to a VirB7::PhoA41 homodimer. A VirB7C24S mutant protein was immunologically undetectable, whereas the corresponding VirB7C24S::PhoA41 derivative accumulated to detectable levels but failed to form dissociable homodimers or mixed dimers with wild-type VirB7. We further report that VirB7-dependent stabilization of VirB9 is correlated with the ability of these two proteins to dimerize via formation of a disulfide bridge between reactive Cys-24 and Cys-262 residues, respectively. Two types of dissociable complexes were visualized: (*i*) a 36-kDa complex corresponding in size to a VirB7/VirB9 heterodimer and (*ii*) an 84-kDa complex corresponding in size to a VirB7/VirB9::PhoA293 heterodimer. A VirB9C262S mutant protein was immunologically undetectable, whereas the corresponding VirB9C262S::PhoA293 derivative accumulated to detectable levels but failed to form dissociable heterodimers with wild-type VirB7. Taken together, these results support a model in which the formation of disulfide cross-linked VirB7 dimers represent critical early steps in the biogenesis of the T-complex transport apparatus.**

Agrobacterium tumefaciens incites tumor formation in susceptible plants by processing and exporting a nucleoprotein complex (T-complex) that likely consists of single-stranded DNA (T-DNA), VirD2, a 5′-capping protein, and VirE2, a single-stranded DNA-binding protein (see ref. 1). Two compelling lines of evidence suggest that *A. tumefaciens* delivers T-complexes to plant cells by a mechanism resembling conjugation (1–3). First, the proposed components of the T-complex transport machinery, at least 10 of the 11 products of the large ~9.5-kilobase *virB* operon (4), exhibit extensive sequence similarities with Tra proteins encoded by the broad host range (BHR) plasmids of the IncN (5), IncP (6), and IncW (7) incompatibility groups. Second, both the presumed *virB*-encoded transport apparatus and the Tra systems of the BHR plasmids promote the conjugal transfer of a common substrate, the non-selftransmissible IncQ plasmid, RSF1010 (8–10). More intriguingly, components of each of these conjugation systems bear sequence similarities with components of the *Bordetella pertussis* Ptl transporter, which directs the export of the six-subunit pertussis toxin to mammalian cells (2, 11). Hence, a family of transporters has been identified that collectively exhibits the ability to export macromolecules as diverse as nucleoprotein particles and multicomponent proteins across the Gram-negative bacterial envelope for delivery to bacterial, plant, or mammalian recipient cells.

Structure/function studies of this family of transporters have led to models describing the possible localizations and interactions of pKM101 Tra (2) and pTi VirB (12) proteins at the bacterial envelope. Among the VirB proteins, the VirB4 and VirB11 ATPases (13, 14) reside at the cytoplasmic face of the cytoplasmic membrane; VirB6 is predicted to be a multispanning cytoplasmic membrane protein; VirB5 and VirB7 through VirB10 are membrane-associated proteins with large periplasmic domains; and VirB1, VirB2, and VirB3 are membrane-associated proteins with periplasmic and/or extracellular domains (1, 2, 12–18). While this information offers important insights about the general organization of this presumed transport system, no data currently exist about specific VirB protein contacts or the process by which this transport system is assembled. In a recent study, we demonstrated that a Δ*virB7* mutant accumulates low levels of several VirB proteins and, furthermore, that modulation specifically of *virB7* expression in trans results in corresponding changes in levels of other VirB proteins (4). Further studies led to a model in which VirB7, an outer membrane-associated lipoprotein (12), acts in conjunction with VirB9 to promote the accumulation of most of the VirB proteins to wild-type levels (4, 19). In the present study, we show that stabilization of both VirB7 and VirB9 is correlated with the abilities of these proteins to form intermolecular disulfide bridges.

MATERIALS AND METHODS

Bacterial Strains, Media, and Growth Conditions. A348 is an *A. tumefaciens* strain A136 containing pTiA6NC (20). The A348 derivatives, PC1007 and PC1009, are nonpolar *virB7* and *virB9* null mutants, respectively (4). The A348 derivative, PC1000, is deleted of the entire 9.5-kb *virB* operon from pTiA6NC (12). Bacterial growth and induction conditions have been described previously (4, 18).

Plasmid Constructions. Plasmids pPCB873 (P_{lac}::*virB7*::*phoA41*) and pPCB992 (P_{lac}::*virB9*) were described previously (4, 12). Plasmid pPCB79, which expresses *virB7* and *virB9* from independent P_{virB} promoters, was constructed by fusing a kanamycin-resistant derivative of pPC974 (4) to the *Pst*I site of pPCB995 (4). Plasmids pXZB14 (P_{lac}::*virB7C24S*) and pXZB15 (P_{lac}::*virB7C24S*::*phoA41*) were constructed as follows. For plasmid pXZB14, we substituted a Ser codon for the

The publication costs of this article were defrayed in part by page charge payment. This article must therefore be hereby marked "*advertisement*" in accordance with 18 U.S.C. §1734 solely to indicate this fact.

Abbreviations: BHR, broad host range; BME, β-mercaptoethanol.

*e-mail: christie@utmmg.med.uth.tmc.edu.

Cys-262 codon of *virB7* by PCR mutagenesis. Plasmid pXZbB7 consists of *virB7* as an *Nde*I–*Bam*HI fragment from pPC978 (4) cloned into corresponding sites of plasmid pAS1 (21). An oligonucleotide containing the Cys-24 to Ser codon substitution (GCCTTTGGAGCTCGCTATTGTG) and an oligonucleotide complementary to sequences residing just upstream of the *Nde*I site were used along with pXZb7 as a template for PCR amplification of 126 bp at the 5′-end of *virB7*. This fragment was used along with the T7 primer to amplify the remaining portion of *virB7* from a pPC978 template. Amplified *virB7C24S* was cloned as an *Nde*I–*Xho*I fragment into pBSIISK$^+$·*Nde*I (4), and the codon substitution was confirmed for plasmid pXZ14 by sequence analysis (DNA Core Facility, UTHSC/H). For plasmid pXZ15, we introduced the 122-bp *Nde*I–*Bgl*II fragment of *virB7C24S* from pXZ14 into pUI1156 (12). These and other ColE1 plasmids described below were ligated to the IncP plasmid, pTJS75-Kan (22), for introduction into *A. tumefaciens* (12, 19). The resulting plasmids were given the names of the corresponding ColE1 plasmids plus B, for Broad host range, i.e., pXZB14 and pXZB15.

Plasmids pXZB21 (P_{lac}::*virB9C262S*), pXZB18 (P_{lac}::*virB9*::*phoA293*), and pXZB19 (P_{lac}::*virB9C262S*::*phoA293*) were constructed as follows. For plasmid pXZB21, we substituted a Ser codon for the Cys-262 codon of *virB9* by PCR mutagenesis. Plasmid pXZaB9 contains *virB9* as an *Nde*I–*Bam*HI fragment from pPCB993 (4) cloned into corresponding sites of pACT2.2 (21). An oligonucleotide containing the Cys-262 to Ser codon substitution (GGCATTCCAGATCGATAGTACTGTGTG) and an oligonucleotide complementary to sequences residing just upstream of the *Nde*I site were used with pXZaB9 as a template to amplify 776-bp of the 5′ end of *virB9*. This fragment was used along with the T7 primer to amplify the remaining portion of *virB9* with pPCB998 (4) as a template. Amplified *virB9C262S* was cloned as an *Nde*I–*Kpn*I fragment into PBSIISK$^+$·*Nde*I (4), and the codon substitution was confirmed for pXZ21 by sequence analysis. For plasmid pXZ18, we fused *'phoA* to the 3′-end of *virB9* by first amplifying the entire *virB9* coding sequence with the M13 reverse primer and an oligonucleotide we previously used to introduce an *Nde*I site at the translation start site of *virB10* (4) with pJW327 (22) as a template. Next, the amplified product was introduced as a *Hin*dIII–*Nde*I (converted to blunt ends with Klenow) fragment into the *Hin*dIII–*Eco*RV sites of pUI1158 (12). For plasmid pXZB19, we amplified the full-length *virB9::C262S* coding sequence with pXZ18 as a template and the primers described for construction of pXZ18. The amplified product was introduced as a *Hin*dIII–*Nde*I (converted to blunt ends with Klenow) fragment into the *Hin*dIII–*Eco*RV sites of pUI1158 (12).

Protein Analysis and Immunological Techniques. Proteins >15 kDa were resolved by glycine SDS/PAGE, and low molecular weight proteins were resolved by *N*-[2-hydroxy-1,1,bis(hydroxymethyl)ethyl]glycine (Tricine) SDS/PAGE as described previously (12, 19). Protein extracts were suspended in reducing [0.125 M Tris·HCl (pH 6.8), 4.6% SDS, 20% glycerol (vol/vol), 10% β-mercaptoethanol (BME) (vol/vol)] or nonreducing (minus BME) protein sample buffers. To ensure that the disulfide bridges detected in these studies were formed *in vivo*, *N*-ethylmaleimide, a thiol-alkylating agent that blocks free sulfhydryl groups and prevents the formation of disulfide bonds (24), was routinely added at a final concentration of 10 mM to cultures immediately prior to cell pelleting. For immunoprecipitation, cells from a 10-ml culture were incubated in 3 ml of spheroplast buffer [25% sucrose, 50 mM Tris·HCl (pH 8.0), 0.5 mg/ml lysozyme, 1.5 mM EDTA] on ice for 15 min. Spheroplasts were disrupted by the addition of 1 volume of 2× lysis buffer [300 mM NaCl, 2% Nonidet P-40, 1.0% deoxycholate, 0.2% SDS, 100 mM Tris·HCl (pH 8.0)] and incubation on ice for 2 h. The cell extract was centrifuged at 14,000 × *g* for 30 min to remove unsolubilized material. Five microliters of antiserum was added to 1 ml of solubilized cell extract followed by incubation on ice for 8 h, and then 2 mg of swollen Sepharose beads coupled to *Staphylococcus aureus* Protein A (Pharmacia) were added followed by incubation on ice for 12 h. Precipitates were recovered by centrifugation of samples at 12,000 × *g* for 5 min at room temperature and analyzed for the presence of VirB proteins by SDS/PAGE and immunostaining as described previously (19).

RESULTS

A348 Cells Accumulate Disulfide Cross-linked VirB7/VirB7 and VirB7/VirB9 Complexes. Immunoprecipitates recovered from A348 cell extracts with anti-VirB7 (12) or anti-VirB9 (22) antisera were suspended in reducing sample buffer, electrophoresed through SDS/polyacrylamide gels using glycine or Tricine buffer systems, and examined immunologically for the presence of a coprecipitating complex of both proteins. Fig. 1 shows that anti-VirB7 antisera (lane 3), but not preimmune sera (lane 4), co-precipitated the monomeric forms of both the VirB7 (4.5 kDa) and VirB9 (32 kDa) proteins (panels *A–C*). Similarly, anti-VirB9 antisera (lane 8), but not preimmune sera (lane 7), co-precipitated both the VirB7 and VirB9 proteins (panels *A–C*). These findings show that VirB7 and VirB9 associate as a tight complex.

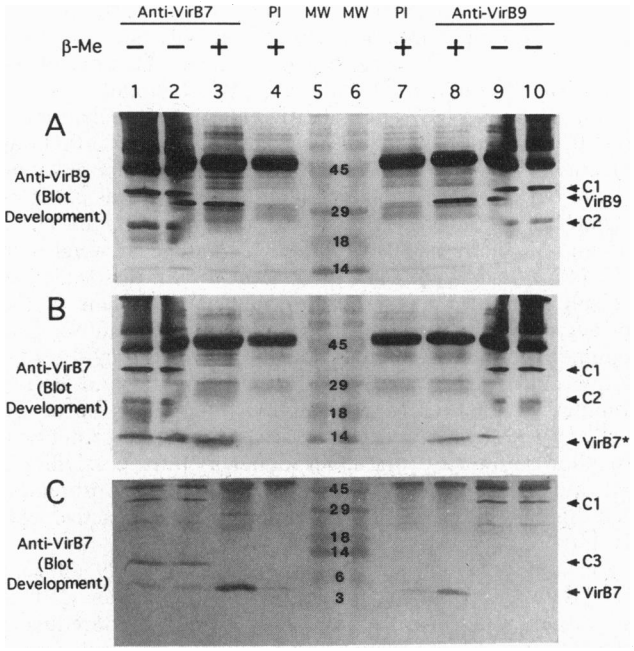

FIG. 1. Immunoblot analysis of material precipitated from A348 extracts with anti-VirB7 and anti-VirB9 antisera. Immunoprecipitates were electrophoresed through glycine- (*A*, *B*) or Tricine- (*C*) polyacrylamide gels and blotted onto nitrocellulose filters. Filters were incubated with anti-VirB9 (A) or anti-VirB7 (*B*, *C*) antisera, and bound antibodies were visualized as described (12, 19). Material recovered by precipitation with anti-VirB7 (lanes 1 and 2) and anti-VirB9 (lanes 9 and 10) antisera suspended in nonreducing (−) protein sample buffer; material recovered with anti-VirB7 (lane 3) and anti-VirB9 (lane 8) antisera suspended in reducing (BME-containing) sample buffer; material recovered with the corresponding preimmune sera (lanes 4 and 7) suspended in reducing sample buffer; molecular mass markers (lanes 5 and 6) with sizes in kDa as indicated. Positions of immunoreactive complexes C1 (VirB7/VirB9 heterodimer), C2 (cross-reactive with anti-VirB7 and anti-VirB9 antisera), C3 (VirB7 homodimer), and monomeric forms of VirB7 and VirB9 are indicated at the right. Assignment of immunoreactive VirB7 species at the dye front of glycine SDS/polyacrylamide gels (*B*) was presumptive (VirB7*) as described in the text. The heavy-staining band at ~45 kDa is due to immunoreactivity of IgG heavy chain present in the immunoprecipitates.

Immunoprecipitates from A348 also were suspended in nonreducing sample buffer and examined by SDS/PAGE and immunostaining for the presence of a complex of VirB7 and VirB9. Fig. 1 shows that these samples possessed very low levels of the VirB7 monomer and undetectable levels of the VirB9 monomer. Instead, the anti-VirB7 and anti-VirB9 antisera each precipitated a 36-kDa species, the size expected of a VirB7/VirB9 heterodimer, that cross-reacted with both antisera in immunoblots (Fig. 1 *A–C*, lanes 1 and 10). This 36-kDa species corresponds to complex C1 identified previously (19). Complex C1 dissociated into VirB9 monomers and, presumptively, VirB7 monomers upon exposure to BME. This was demonstrated by electrophoresis of immunoprecipitates suspended in reducing and nonreducing sample buffers in adjacent lanes of a glycine SDS/12.5% polyacrylamide gel. Diffusion of BME through the gel caused the region of complex C1 located proximal to the BME-containing lane to dissociate into the VirB9 monomer and the presumptive VirB7 monomer. The region of complex C1 located distal to the BME-containing lane remained intact (Fig. 1 *A* and *B*, lanes 2 and 9). Although complex C1 dissociated into an immunoreactive VirB7 species, the assignment of this species as the monomeric form of VirB7 was presumptive because the glycine SDS/12.5% polyacrylamide gels resolved proteins > ~15 kDa. With Tricine SDS/PAGE, we observed no dissociation of complexes as a result of diffusion of BME. Thus, our conclusion that monomeric VirB7 is a component of complex C1 is based on: (*i*) co-precipitation and co-reactivity of complex C1 with VirB7 and VirB9 antisera and (*ii*) a size difference of ~4 kDa between complex C1 and the VirB9 monomer.

Both the anti-VirB7 and anti-VirB9 antisera precipitated a second, less prominent species designated complex C2 that was detectable only in precipitates suspended in nonreducing sample buffer (Fig. 1 *A* and *B*, lanes 1 and 9). This complex migrated as a doublet of bands, each reactive with anti-VirB7 and anti-VirB9 antisera, with apparent molecular weights of ~19 and 20 kDa. Complex C2 also was partially dissociated as a result of diffusion of BME from an adjacent lane of the polyacrylamide gel (Fig. 1 *A* and *B*, lanes 2 and 9). The immunological cross-reactivity of this complex provides suggestive evidence that it is comprised of VirB7 and VirB9. Complex C2 may represent a partially-unfolded form of the VirB7/VirB9 heterodimer, or, alternatively, a proteolytic breakdown product of the heterodimer. A third possibility is that complex C2 consists of VirB7 linked to another protein(s) such that an epitope of the resulting complex is reactive with the anti-VirB9 antisera.

The anti-VirB7 antisera but not the anti-VirB9 antisera precipitated a prominent species designated complex C3 that was present only in precipitates suspended in nonreducing sample buffer (Fig. 1 *C*, lanes 1 and 2). This complex migrated as a ~9-kDa species, the size expected of a VirB7 homodimer, and reacted only with VirB7 antisera. It is noteworthy that only a very small amount of the ~4.5-kDa monomeric form of VirB7 was detected in immunoprecipitates electrophoresed under nonreducing conditions. These findings suggest that VirB7 exists *in vivo* exclusively as a homodimer or as a heterodimer with VirB9.

PC1000(pPCB79) Cells Accumulate Disulfide Cross-linked VirB7/VirB7 and VirB7/VirB9 Complexes. We next examined whether the presumptive VirB7 homodimer and the VirB7/VirB9 heterodimer assemble in PC1000, a Δ*virB* operon derivative of A348 (12) containing pPCB79 that expresses *virB7* and *virB9* from a P_{lac} promoter. Fig. 2 shows that material recovered from extracts of strain PC1000(pPCB79) by precipitation with VirB7 and VirB9 antisera possessed VirB7 and VirB9 monomers when electrophoresed under reducing conditions (Fig. 2 *A–C*, lanes 3 and 8). Furthermore, immunoprecipitates possessed complexes C1 and C3 when electrophoresed under nonreducing conditions (lanes 1 and 10). Complexes C1 and C3 also were dissociated upon diffusion of BME from adjacent gel lanes (Fig. 2 *A* and *B*, lanes 2 and 9). Again, the monomeric form of VirB9 clearly was shown to be a component of complex C1 (Fig. 2*A*, lanes 2 and 9), whereas the assignment of VirB7 to this complex rests on immunological cross-reactivity and co-precipitation of complex C1 with anti-VirB7 and anti-VirB9 antisera and a 4-kDa size difference between complex C1 and monomeric VirB9 (Fig. 2 *A–C*). Results of these studies show that VirB7 and VirB9 assemble as covalent dimers independent of other VirB proteins.

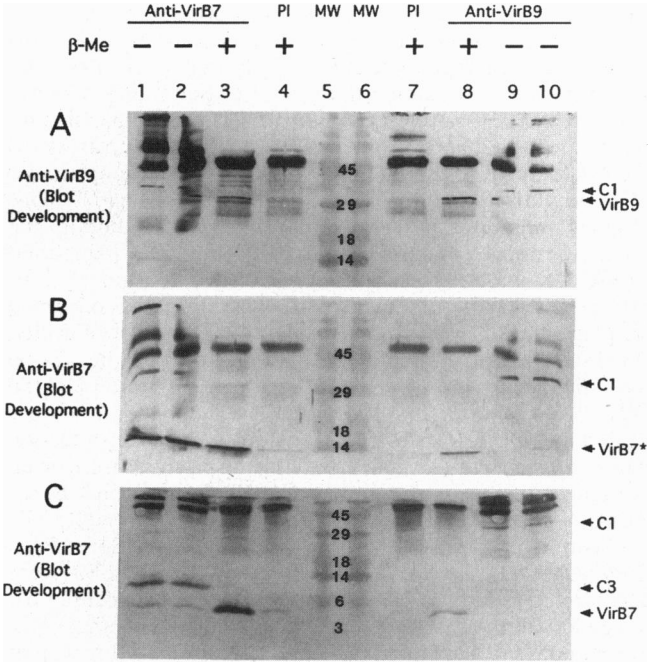

FIG. 2. Immunoblot analysis of material precipitated from PC1000(pPCB79) extracts with anti-VirB7 and anti-VirB9 antisera. Immunoprecipitates were electrophoresed through glycine- (*A*, *B*) or tricine- (*C*) polyacrylamide gels, and blotted onto nitrocellulose filters. Filters were incubated with anti-VirB9 (*A*) or anti-VirB7 (*B*, *C*) antisera, and bound antibodies were visualized as described (12, 19). Lanes are as described in Fig. 1. Positions of immunoreactive complexes C1 and C3 (see Fig. 1 legend) and monomeric forms of VirB7 and VirB9 are indicated at the right.

Cys-24 Is the Reactive Cysteine of VirB7. VirB7 from pTiA6NC possesses four cysteines (25, 26), two in its cleaved signal sequence, an amino-terminal Cys-15 residue, which is predicted to be unavailable for intermolecular cross-linking (12, 27), and an internal Cys-24 residue. We examined the effect of a Cys-24 to Ser substitution on the ability of VirB7 to form dissociable complexes. As also shown above, A348 extracts suspended in reducing sample buffer possessed monomeric forms of VirB7 and VirB9 (Fig. 3 left panels, lanes 1 and 3), and the corresponding nonreduced samples possessed complexes C1, C2, and C3 (Fig. 3 right panels, lanes 1 and 3). By contrast, BME-treated extracts of the Δ*virB7* mutant, PC1007, expressing the *virB7C24S* allele from pXZB14 possessed undetectable levels of VirB7C24S (Fig. 3 left panels, lane 2). PC1007 cells expressing wild-type *virB7* in trans possess abundant levels of VirB7 (19). The nonreduced samples from PC1007(pXZB14) cells also possessed undetectable levels of complexes C1, C2, and C3 (Fig. 3 right panels, lane 2). These findings implicate Cys-24 as the reactive cysteine required for formation of intermolecular disulfide bonds. Furthermore, dimerization appears to be correlated with stabilization of VirB7. However, an alternative explanation is that the C24S mutation destabilizes VirB7 for reasons unrelated to dimerization. To distinguish these possibilities, we sought to stabilize VirB7C24S to then determine whether the mutant

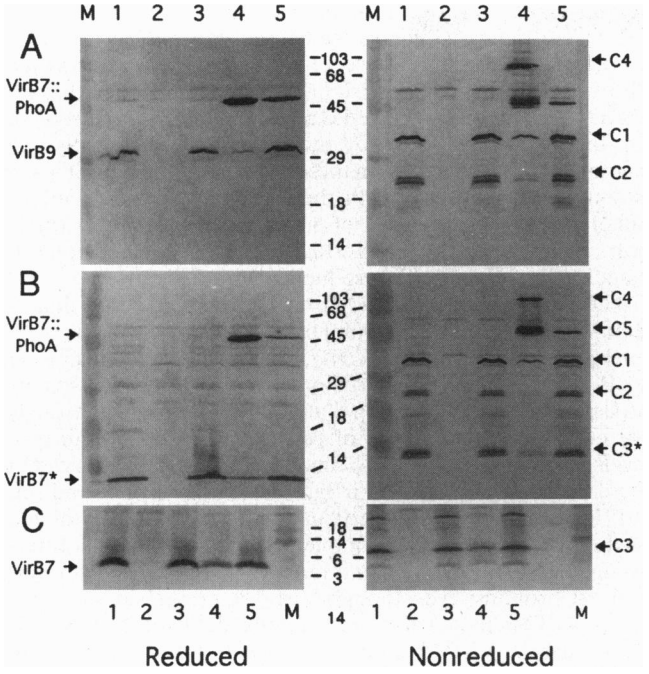

FIG. 3. Immunoblot analysis of total protein extracts electrophoresed under reducing (left panels) and nonreducing (right panels) conditions. The corresponding nitrocellulose filters were incubated with anti-VirB9 (*A*) or anti-VirB7 (*B*, *C*) antisera. Protein samples were from wild-type A348 (lanes 1 and 3), PC1007(pXZB15) (lanes 2); A348(pPCB873) (lanes 4); and A348(pPXZB15) (lane 5); molecular mass markers (M) with sizes in kDa indicated between the left and right panels. Positions of the immunoreactive complexes C1-C3 (See Fig. 1 legend), C4 (VirB7::PhoA41 homodimer), and C5 (VirB7/VirB7::PhoA41 mixed dimer) are indicated at the right and the monomeric forms of VirB7, VirB7::PhoA41, and VirB9 at the left. Assignment of complex C3 at the dye front of glycine SDS/polyacrylamide gels (*B*) was presumptive (C3*).

protein forms intermolecular cross-links. The first objective was achieved by fusing VirB7C24S to PhoA, which itself is stabilized in the periplasm by formation of noncovalent dimers (28).

Initial experiments showed that the unmutated VirB7 derivative, VirB7::PhoA41, formed two dissociable complexes in A348(pPCB873) cells that express *virB7::phoA41* from the P_{lac} promoter (12). A complex designated C4 migrated at a position corresponding to ~102 kDa, the size expected of a VirB7::PhoA41 homodimer. Both anti-VirB7 (Fig. 3*B*, lane 4) and anti-PhoA (data not shown) antisera reacted with complex C4. Although our anti-VirB9 antisera also reacted with this complex (Fig. 3*A*, left panels, lane 4), we have determined that this is due to the presence of contaminating PhoA antibodies present in these sera (data not shown). Furthermore, strain PC1009, a Δ*virB9* mutant, carrying pPCB873 accumulated abundant levels of complex C4, providing definitive evidence that VirB9 is not a component of complex C4 (data not shown). The complex designated C5 migrated at a position corresponding to ~55 kDa, ~4 kDa larger than the monomeric form of the 51-kDa VirB7::PhoA41 fusion protein. Complex C5 was not immunologically detectable in PC1007(pPCB873) extracts but was visualized in extracts of other *virB* gene deletion strains transformed with pPCB873 (data not shown). Therefore, complex C5 corresponds to a mixed dimer of VirB7 and VirB7::PhoA41. We failed to detect an ~83-kDa complex, the expected size of a VirB9/VirB7::PhoA41 heterodimer, possibly because the PhoA moiety sterically hinders formation of such a complex.

A348(pPXZB15) cells possessed abundant levels of a ~51-kDa VirB7C24S::PhoA41 fusion protein, clearly showing that the PhoA moiety stabilizes the C24S mutant protein (Fig. 3*B*, left panels, lane 5). The corresponding nonreduced extracts possessed undetectable levels of complexes C4 and C5, the presumptive VirB7::PhoA41 homodimer and VirB7/VirB7::PhoA41 mixed dimer (Fig. 3*B*, right panels, lane 5). Together, these data establish: (*i*) Cys-24 of VirB7 is directly involved in the formation of dissociable homodimers and dimers consisting of VirB7 and VirB7::PhoA41 and (*ii*) dimerization is strongly correlated with stabilization of VirB7.

Cys-262 Is the Reactive Cysteine Residue of VirB9. VirB9 from pTiA6NC possesses two cysteines (25, 26), one in its cleaved signal sequence and Cys-262. We examined the effect of a Cys-262 to Ser substitution on heterodimer formation. Nonreduced extracts of both A348 and PC1009 cells expressing *virB9* from pPCB992 (4) possessed complexes C1 and C2 (Fig. 4 *A* and *B*, right panels, lanes 1 and 3). By contrast, nonreduced extracts of PC1009(pXZB21) cells expressing the *virB9C262S* allele possessed undetectable levels of complexes C1 and C2 (Fig. 4*A*, right panels, lane 2). The corresponding BME-treated extracts of PC1009(pXZB21) cells also possessed undetectable levels of VirB9C262S (Fig. 4*A*, left panels, lane 2). These findings implicate Cys-262 as the reactive cysteine required for formation of intermolecular disulfide bonds.

We fused VirB9C262S to PhoA to test whether a stabilized VirB9C262SS derivative was able to form intermolecular cross-links. A348 cells expressing *virB9::phoA293* from pXZB18 possessed complex C1, the VirB7/VirB9 heterodimer, and a complex designated C6 that migrated at a position corresponding to ~85 kDa, the size expected of a VirB7/VirB9::PhoA293 heterodimer (Fig. 4 *A* and *B*, right panels, lane 5). Both anti-VirB7 (Fig. 4*B*) and anti-VirB9 antisera (Fig. 4*A*) reacted with complex C6. Our VirB7 antisera do not possess contaminating PhoA antibodies (data not shown). Complex C6 dissociated into the monomeric form of VirB9::PhoA293 as a result of diffusion of BME through the SDS-polyacrylamide gel. This appeared as a band exhibiting immunoreactivity to anti-VirB9 but not to anti-VirB7 antisera that migrated just below the C6 complex (Fig. 4*A*, right panels, lane 6) and co-migrated with the monomeric form of VirB9::PhoA293 present in the corresponding β-mercaptoethanol-treated samples (Fig. 4*A*, right panels, lane 7). These

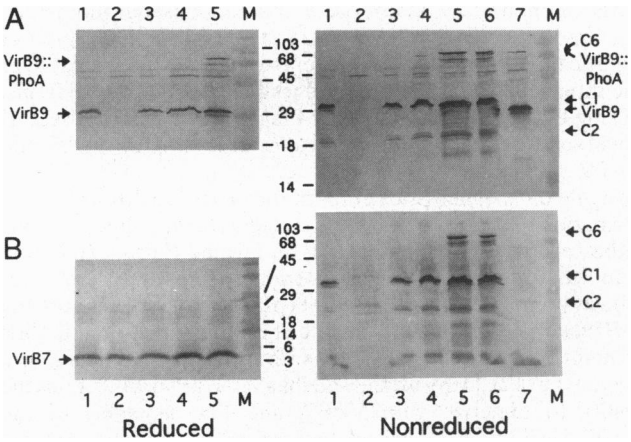

FIG. 4. Immunoblot analysis of total protein extracts electrophoresed under reducing (left panels) and nonreducing (right panels) conditions. The corresponding nitrocellulose filters were incubated with anti-VirB9 (*A*) or anti-VirB7 (*B*) antisera. Protein samples were from wild-type A348 (lanes 1); PC1009(pXZB21) (lanes 2); PC1009(pPCB992) (lanes 3); A348(pXZB19) (lanes 4); A348(pXZB18) (lanes 5–7). Proteins from A348(pXZB18) were suspended in nonreducing (lanes 5 and 6) and reducing (lane 7) sample buffers; molecular mass markers (M) with sizes in kDa indicated between the left and right panels. Positions of the immunoreactive complexes C1and C2 (see Fig. 1 legend) and C6 (VirB7/VirB9::PhoA293) are indicated at the right and the monomeric forms of VirB7, VirB7::PhoA41, and VirB9 at the left.

findings show that VirB7 forms a dissociable cross-link both with VirB9 and VirB9::PhoA293.

A348 cells expressing *virB9C262::phoA293* from pXZB19 possessed detectable levels of the VirB9C262S::PhoA293 fusion protein, showing that the PhoA moiety stabilizes the C262S mutant protein (Fig. 4*A*, left and right panels, lane 4). VirB9C262S::PhoA293 migrated at a position slightly lower than that of complex C6 (Fig. 4*A*, right panels, lanes 4 and 5), and exhibited reactivity with anti-VirB9 but not anti-VirB7 antisera. Thus, in contrast to VirB9::PhoA293, VirB9C262S::PhoA293 fails to form a disulfide bridge with VirB7. Together, these data establish: (*i*) Cys-262 of VirB9 is required for formation of VirB7/VirB9 heterodimers and (*ii*) dimerization is strongly correlated with stabilization of VirB9.

DISCUSSION

Our studies indicate that two biochemical pathways must converge for assembly of the T-complex transport machinery. The first pathway directs the export and maturation of VirB7 as a lipoprotein (12), most probably according to a biosynthetic pathway developed for Lpp, the major outer membrane lipoprotein of *Escherichia coli* (27). The second pathway, identified in this study, is postulated to function in the stabilization of VirB7 and VirB9 monomers by catalyzing formation of disulfide cross-linked VirB7 homodimers and VirB7/VirB9 heterodimers. The enzymes responsible for catalyzing formation of intermolecular disulfide bonds likely are functional analogs of the Dsb (Disulfide bond formation) proteins recently identified in *E. coli* and other species (see ref. 29). These thiol/disulfide interchange proteins catalyze the formation of intramolecular disulfide bonds in a wide variety of exported proteins, including secreted exotoxins (30) and components of several eubacterial macromolecular surface structures such as *E. coli* flagella (31), *Vibrio cholerae* toxin-coregulated colonization pilus (32), and the *Haemophilus influenzae* competence system (33). Interestingly, we have recently discovered that *E. coli* DH5α cells expressing *virB7* only or *virB7* together with *virB9* fail to assemble VirB7 homodimers or VirB7/VirB9 heterodimers, respectively (X.-R. Zhou and P. J. Christie, unpublished data). These findings confirm that cross-linking of VirB7 monomers does not occur spontaneously in the oxidizing environment of the eubacterial periplasm. Of greater significance, the *E. coli* Dsb proteins apparently do not catalyze the intermolecular disulfide bridges formed in *A. tumefaciens*, raising the intriguing possibility that *A. tumefaciens* possesses novel oxidoreductase/isomerases for cross-linking VirB7 and VirB9 monomers.

While the mechanistic details of the proposed disulfide bond formation pathway remain to be elucidated, three lines of study indicate that VirB7 dimers must be formed for assembly of a stabilized, functional T-complex transport apparatus. We previously demonstrated that A348(pPCB873) cells expressing *virB7::phoA41* in trans accumulate aberrantly low levels of VirB proteins (ref. 19; see Fig. 3) and a severely-attenuated virulence phenotype (19). Here, we showed that VirB7::PhoA41 retains the ability to dimerize with VirB7, and that assembly of the VirB7/VirB7::PhoA41 mixed dimer is strongly correlated with a significant reduction in steady-state levels of the VirB7 homodimer as well as the VirB7/VirB9 heterodimer (Fig. 3). Furthermore, A348(pXZB15) cells expressing *virB7C24S* in trans accumulate wild-type levels of VirB7 and VirB9, as well as complexes C1, C2, and C3, demonstrating that VirB7::PhoA41 must perturb steady-state levels of VirB proteins through its ability to form disulfide cross-linked dimers (Fig. 3). These observations could be explained in three ways: (*i*) Formation of the VirB7/VirB7::PhoA41 mixed dimer inhibits assembly of the VirB7 homodimer as well as the VirB7/VirB9 heterodimer by titrating newly-secreted VirB7 monomers, (*ii*) VirB7::PhoA41 dimerizes with VirB9, but the mixed dimers are unstable, and, hence, undetectable by immunostaining; this mixed dimer inhibits assembly of the VirB7/VirB9 heterodimer by titrating newly-secreted VirB9 monomers; (*iii*) the PhoA moiety of VirB7/VirB7::PhoA41 or the hypothetical VirB9/VirB7::PhoA41 mixed dimer presents a steric problem for the further assembly of the transporter. Presently, we cannot discriminate between these possibilities. However, each is consistent with the notion that the VirB7::PhoA41 mixed dimer(s) impedes assembly of a functional T-complex transport apparatus at an early stage in the assembly process, namely, the formation of productive VirB7 dimers.

The next two lines of study provided evidence that dimerization is critical for T-complex transporter assembly and, furthermore, that it is the VirB7/VirB9 heterodimer, not the VirB7 homodimer, that participates directly in this assembly process. First, we have shown that synthesis of VirB9 is strongly correlated with the ability of cells to accumulate wild-type levels of other VirB proteins. Since VirB9 itself is stabilized in the context of the VirB7/VirB9 heterodimer (Fig. 4 and ref. 19), formation of this heterodimer must be required for the further assembly of the T-complex transport apparatus. Interestingly, a nonpolar *virB9* null mutant accumulates low levels of VirB proteins, even though VirB7 is present at wild-type levels (4, 19) in the form of homodimers (data not shown). This shows that the VirB7 homodimer by itself does not contribute to the stabilization of VirB proteins.

Second, the immunoprecipitation studies showed that A348 cells accumulate abundant levels of the VirB7/VirB9 heterodimer and low levels of the VirB7 homodimer (Fig. 1). Conversely, PC1000(pPCB79) cells accumulate abundant levels of the VirB7 homodimer and low levels of the VirB7/VirB9 heterodimer (Fig. 2). Thus, the VirB7/VirB9 heterodimer and other VirB proteins appear to be mutually stabilizing, most likely as a result of their association in a functional transport apparatus. By contrast, the VirB7 homodimer neither stabilizes nor is stabilized by other VirB proteins. Together, our findings raise the interesting question of whether the VirB7 homodimer plays any physiological role in T-complex transport. One possibility that warrants further study is that the VirB7 homodimer functions exclusively as an intermediate in a disulfide bond formation pathway dedicated to assembly of the productive VirB7/VirB9 heterodimer.

The observed stabilizing activities of VirB7 and VirB9 on other VirB proteins argues strongly that once the VirB7/VirB9 heterodimer is properly positioned at the *A. tumefaciens* envelope, the heterodimer functions as a nucleation center for the assemblage of VirB proteins into a functional T-complex transport apparatus. We have gained some insights into possible stabilizing contacts between the VirB7/VirB9 heterodimer and other VirB proteins. *A. tumefaciens* cells expressing *virB7* and *virB8* from an isopropyl-1-thio-β-D-galactopyranoside-inducible P_{lac} promoter and *virB9*, *virB10*, and *virB11* from the acetosyringone-inducible P_{virB} promoter accumulate VirB9, VirB10, and VirB11 in rough proportion to the amount of VirB7 detected in these cells (19). This finding formed the basis of a prediction that the VirB7/VirB9 heterodimer interacts with VirB10 and VirB11 (19). Beaupre and Binns (C. Beaupre and A. N. Binns, personal communication) also proposed that VirB9 interacts with VirB10 based on their observation that synthesis of VirB9 influences the oligomeric state of VirB10. VirB7, VirB9, and VirB10 are membrane-associated proteins with large periplasmic domains, consistent with the notion that these proteins directly interact (12, 15–17). By contrast, VirB11 as well as VirB4, a second ATPase whose steady-state levels also are influenced by synthesis of VirB7, are cytoplasmic membrane-bound proteins that most probably reside predominantly or exclusively within the cell interior (13, 18). This suggests that the stabilizing effect of the VirB7/VirB9 heterodimer on these two ATPases is mediated through another cytoplasmic membrane-spanning VirB protein, pos-

sibly VirB10, a predicted monotopic protein with an amino-terminal cytoplasmic membrane-spanning domain (16).

Are features of the T-complex transporter assembly pathway identified in our investigations (12, 19, this study) also prominent in assembly pathways for other conjugal DNA transporters or, more broadly, other macromolecular surface structures? Their unique mode of attachment to the bacterial membrane (27), coupled with fact that lipoproteins are associated with many eubacterial surface structures (see ref. 19), is at least consistent with the possibility that lipoproteins contribute essential stabilization functions during assembly processes. Also, as noted above, there are numerous examples in which the formation of intramolecular disulfide bonds promotes the correct folding of polypeptide constituents of eubacterial surface structures (29–33). Intermolecular disulfide bridges likely promote the correct folding of interactive polypeptides; hence, it seems reasonable that intermolecular disulfide bridges also play prominent roles in macromolecular assembly processes. Interestingly, however, although both VirB7 proteins from pTiA6NC and pTiC58 as well as possible functional analogs of VirB7, i.e., PtlI from *B. pertussis* (2) and TrbH from the IncP plasmid, RP4α (6), possess potentially-reactive internal cysteine residues, other VirB7 homologs or analogs, i.e., the TraN protein from the IncN plasmid, pKM101 (5), and the Bacteriocin Release Proteins lipoproteins encoded by the colicinogenic plasmids (34), are devoid of internal cysteine residues. The observed sequence similarities of components of the VirB, Ptl, and BHR Tra transport systems and the functional-relatedness of the VirB and BHR Tra systems (1–3) strongly suggests that each of the VirB7-like proteins supplies a conserved function with respect to the assembly/function of the cognate transporter. If so, these lipoproteins play similar roles when assembled as covalent dimers or as noncovalent oligomers or monomers. Perhaps VirB7 acquired the ability to form disulfide cross-links as the result of a fortuitous event during its evolution from a progenitor lipoprotein—the incorporation of a Cys residue by mutation. It is important to note, however, that while the acquisition of an appropriately-positioned Cys residue was an essential prerequisite for assembly of these disulfide bridges, a dedicated pathway must also have evolved to catalyze their formation. Interestingly, this pathway appears to be present and functional in *A. tumefaciens* but not in *E. coli*.

We thank Drs. Anath Das and Christian Baron for communication of results prior to publication. We thank Drs. Heidi Kaplan and John Spudich for critical review of this manuscript. This work was supported by Public Health Service Grant GM48746.

1. Zupan, J. R. & Zambryski, P. (1995) *Plant Physiol.* **107,** 1041–1047.
2. Winans, S. C., Burns, D. L. & Christie, P. J. (1996) *Trends Microbiol.* **4,** 64–68.
3. Lessl, M. & Lanka, E. (1994) *Cell* **77,** 321–324.
4. Berger, B. R. & Christie, P. J. (1994) *J. Bacteriol.* **176,** 3646–3660.
5. Pohlman, R. F., Genetti, H. D. & Winans, S. C. (1994) *Mol. Microbiol.* **14,** 655–668.
6. Lessl, M., Balzer, D., Pansegrau, W. & Lanka, E. (1992) *J. Biol. Chem.* **267,** 20471–20480.
7. Kado, C. I. (1993) in *Bacterial Conjugation*, ed. Clewell, D. B. (Plenum, New York), pp. 243–254.
8. Beijersbergen, A., Dulk-Ras, A. D., Schilperoort, R. A. & Hooykaas, P. J. J. (1992) *Science* **256,** 1324–1327.
9. Haase, J., Lurz, R., Grahn, A. M., Bamford, D. H. & Lanka, E. (1995) *J. Bacteriol.* **177,** 4779–4791.
10. Buchanon-Wollaston, V., Passiatore, J. E. & Cannon, F. (1987) *Nature (London)* **328,** 172–175.
11. Weiss, A. A., Johnson, F. D. & Burns, D. L. (1993) *Proc. Natl. Acad. Sci. USA* **90,** 2970-2974.
12. Fernandez, D., Dang, T. A. T., Spudich, G. M., Zhou, X.-R. & Christie, P. J. (1996) *J. Bacteriol.* **178,** 3156–3167.
13. Christie, P. J., Ward, J. E., Jr., Gordon, M. P. & Nester, E. W. (1989) *Proc. Natl. Acad. Sci. USA* **86,** 9677–9681.
14. Jones, A. L., Shirasu, D. & Kado, C. I. (1994) *J. Bacteriol.* **176,** 5255–5261.
15. Thorstenson, Y. R., Kuldau, G. A. & Zambryski, P. C. (1993) *J. Bacteriol.* **175,** 5233–5241.
16. Ward, J. E., Jr., Dale, E. M., Nester, E. W. & Binns, A. N. (1990) *J. Bacteriol.* **172,** 5200–5210.
17. Shirasu, K. & Kado, C. I. (1993) *FEMS Microibol. Lett.* **111,** 287–294.
18. Berger, B. R. & Christie, P. J. (1993) *J. Bacteriol.* **175,** 1723–1734.
19. Fernandez, D., Spudich, G. M., Zhou, X.-R. & Christie, P. J. (1996) *J. Bacteriol.* **178,** 3168–3176.
20. Garfinkel, D. J., Simpson, R. B., Ream, L. W., White, F. F., Gordon, M. P. & Nester, E. W. (1981) *Cell* **27,** 143–153.
21. Bai, C. & Elledge, S. J. (1995) *Methods Enzymol.* **273,** 331–347.
22. Ward, J. E., Jr., Dale, E. M., Christie, P. J., Nester, E. W. & Binns, A. N. (1990) *J. Bacteriol.* **172,** 5187–5199.
23. Christie, P. J., Ward, J. E., Winans, S. C. & Nester, E. W. (1988) *J. Bacteriol.* **170,** 2659–2667.
24. Riordan, J. F. & Vallee, B. L. (1972) *Methods Enzymol.* **25,** 449–456.
25. Ward, J. E., Jr., Akiyoshi, D. E., Regier, D., Datta, A., Gordon, M. P. & Nester, E. W. (1988) *J. Biol. Chem.* **263,** 5804–5814.
26. Ward, J. E., Jr., Akiyoshi, D. E., Regier, D., Datta, A., Gordon, M. P. & Nester, E. W. (1990) *J. Biol. Chem.* **265,** 4768.
27. Hayashi, S. & Wu, H. C. (1990) *J. Bioenerg. Biomembr.* **22,** 451–471.
28. Wanner, B. L. (1987) in *Escherichia coli and Salmonella typhimurium. Cellular and Molecular Biology*, ed., Neidhardt, F. C., (American Society for Microbiology, Washington, DC) pp. 1326–1333.
29. Bardwell, J. C. A. (1994) *Mol. Microbiol.* **14,** 199–205.
30. Yu, J., Webb, H. & Hirst, T. R. (1992) *Mol. Microbiol.* **6,** 1949–1958.
31. Dailey, F. E. & Berg, H. E. (1993) *Proc. Natl. Acad. Sci. USA* **90,** 1043–1047.
32. Peek, J. A. & Taylor, R. K. (1992) *Proc. Natl. Acad. Sci. USA* **89,** 6210–6214.
33. Tomb, J. F. (1992) *Proc. Natl. Acad. Sci. USA* **89,** 10252–10256.
34. De Graaf, F. K. & Oudega, B. (1986) *Curr. Top. Microbiol. Immunol.* **125,** 183–205.